



Structural-Guided Identification of Small Molecule Inhibitor of UHRF1 Methyltransferase Activity

Md Abdul Awal¹, Suza Mohammad Nur¹, Ali Khalaf Al Khalaf¹, Mohd Rehan², Amir Ahmad³, Salman Bakr I. Hosawi¹, Hani Choudhry^{1,4} and Mohammad Imran Khan^{1,4*}

¹Department of Biochemistry, Faculty of Science, King Abdulaziz University, Jeddah, Saudi Arabia, ²King Fahd Medical Research Centre, King Abdulaziz University, Jeddah, Saudi Arabia, ³Translational Research Institute, Hamad Medical Corporation, Doha, Qatar, ⁴Centre of Artificial Intelligence for Precision Medicines, King Abdulaziz University, Jeddah, Saudi Arabia

OPEN ACCESS

Edited by:

Hifzur R. Siddique,
Aligarh Muslim University, India

Reviewed by:

Maqsood Ahamed,
King Saud University, Saudi Arabia
Safendri Ragamustari,
Indonesian Institute of Sciences,
Indonesia

*Correspondence:

Mohammad Imran Khan
mikh@kau.edu.sa

Specialty section:

This article was submitted to
RNA,
a section of the journal
Frontiers in Genetics

Received: 26 April 2022

Accepted: 17 June 2022

Published: 03 August 2022

Citation:

Awal MA, Nur SM, Al Khalaf AK, Rehan M, Ahmad A, Hosawi SBI, Choudhry H and Khan MI (2022) Structural-Guided Identification of Small Molecule Inhibitor of UHRF1 Methyltransferase Activity. *Front. Genet.* 13:928884. doi: 10.3389/fgene.2022.928884

Ubiquitin-like containing plant homeodomain Ring Finger 1 (UHRF1) protein is recognized as a cell-cycle-regulated multidomain protein. UHRF1 importantly manifests the maintenance of DNA methylation mediated by the interaction between its SRA (SET and RING associated) domain and DNA methyltransferase-1 (DNMT1)-like epigenetic modulators. However, overexpression of UHRF1 epigenetically responds to the aberrant global methylation and promotes tumorigenesis. To date, no potential molecular inhibitor has been studied against the SRA domain. Therefore, this study focused on identifying the active natural drug-like candidates against the SRA domain. A comprehensive set of *in silico* approaches including molecular docking, molecular dynamics (MD) simulation, and toxicity analysis was performed to identify potential candidates. A dataset of 709 natural compounds was screened through molecular docking where chicoric acid and nystose have been found showing higher binding affinities to the SRA domain. The MD simulations also showed the protein ligand interaction stability of and *in silico* toxicity analysis has also showed chicoric acid as a safe and nontoxic drug. In addition, chicoric acid possessed a longer interaction time and higher LD50 of 5000 mg/kg. Moreover, the global methylation level (%5 mC) has been assessed after chicoric acid treatment was in the colorectal cancer cell line (HCT116) at different doses. The result showed that 7.5 μ M chicoric acid treatment reduced methylation levels significantly. Thus, the study found chicoric acid can become a possible epidrug-like inhibitor against the SRA domain of UHRF1 protein.

Keywords: UHRF1, SRA domain, chicoric acid, global methylation (5 mC), molecular docking, molecular dynamics simulation

INTRODUCTION

The DNA methylation like epigenetic modification in the CpG island manifests a crucial role in mammalian genomic architecture, genomes expression, and genome stability (Chen et al., 1998; Bird and Wolffe, 1999). Moreover, diverse biological responses including tumorigenesis are associated with multiple patterns of DNA methylation (Arita et al., 2008). Among several epigenetic modulators, the DNA methyltransferase family (DNMT) is one of the key components that play with epigenetic modification. It is well established that DNMT1 acts as a canonical epigenetic 'writer' (Patnaik et al., 2018) in the DNA methylation mechanism (Moore et al., 2012). Additionally, DNMT1 incorporates methyl group at the fifth position of cytosine in CpG islands and synthesizes 5-

methylcytosine (5 mC). Moreover, DNMT1 maintains DNA methylation during the DNA replication phase (Pradhan and Esteve, 2003). In contrast, aberrant DNA hypomethylation and hypermethylation are associated with transcriptional activation and repression of gene expression, respectively (Baylin et al., 2001; Patnaik et al., 2018).

Ubiquitin-like containing PHD Ring Finger 1 (UHRF1) is an essential partner protein of DNA methyltransferase and is also known as Np95 (Nuclear Protein 95 KDa) and ICBP90 (Inverted CCAAT box-binding Protein of 90 KDa) in mouse and human, respectively (Veland and Chen, 2017). Structurally, UHRF1 is a complex of distinct domains that include-SRA (SET and RING-associated) domain, a ubiquitin-like (UBL) domain, a plant homeodomain (PHD) domain, and a RING domain (Bostick et al., 2007; Bronner et al., 2007; Sharif et al., 2007; Zhang et al., 2011; Cheng et al., 2013). Moreover, UHRF1 belonging SRA domain recognizes the hemimethylated sequence in DNA and facilitates the DNMT1 binding, thus the maintenance of DNA methylation dynamics (Bostick et al., 2007).

The genomic abundance of DNA methylation disturbs normal cell division and complies with the pathogenic responses (Kong et al., 2019). It has been revealed that UHRF1 can regulate the DNA methylation in both normal and tumor cells by providing accompanying to the epigenetic writer- DNMT1 (Bostick et al., 2007; Sharif et al., 2007; Liao et al., 2015; Cai et al., 2017). Moreover, aberrant DNA methylation leads the alteration of the gene expression and has been considered as a fundamental regulator of tumor progression (Baylin and Jones, 2016). Moreover, global hypermethylation dictates cell proliferation in tumorigenesis through silencing tumor suppressor genes (TSGs) and its promoter (Shen and Laird, 2013; Baylin and Jones, 2016). Previous studies also revealed that UHRF1 protein is expressed during cellular propagation and can regulate the cell cycle (Bonapace et al., 2002; Patnaik, Estève and Pradhan, 2018). Moreover, another study also revealed that the expression of UHRF1 is required by the cell during for S-phase (Bonapace et al., 2002). However, G0/G1 phases may not notably require the UHRF1 (Uemura et al., 2000; Miura et al., 2001). UHRF1 protein is also found to be highly expressed in cancer cells across the cell cycle. For example, the overexpression of UHRF1 has been reported in several cancer-cell like-gastric, bladder, breast, lung, prostate, pancreatic, and colorectal cancer (Crnogorac-Jurcevic et al., 2005; Unoki et al., 2010; Jazirehi, Arle and Wenn, 2012; Kofunato et al., 2012; Li et al., 2012; Yang et al., 2012; Zhou et al., 2013).

Moreover, the study also revealed that overexpression of UHRF1 is associated with the DNA methylation-mediated silencing of tumor suppressor genes (Beck et al., 2018). A study also showed that by recruiting several repressor enzymes, such as DNA methyltransferase 1 (DNMT1), histone deacetylase 1 (HDAC1), and histone lysine methyltransferases, i.e., G9a and Suv39H1, UHRF1 mediates the gene silencing mechanism (Alhosin et al., 2016). Additionally, UHRF1 has been substantially justified for chemotherapeutic targets (Unoki, 2011).

Chemotherapeutic resistance is a bottleneck problem in modern cancer therapies. The chemo-resistance is influenced

through several mechanisms such as chemo target alterations, signaling pathway diversion, and the inactivation of cell death (Holohan et al., 2013; Ahamed et al., 2022). The chemoresistance is explored either by the innate response which is raised through pre-existing factors in tumor cells or by the adaptive response due to mutated expression of molecular target and therapeutic insensitivity to the target (Longley and Johnston, 2005; Ahamed et al., 2021). Likewise, epigenetic modifications of histone, such as acetylation and methylation, generate a range of drug insensitivity (Housman et al., 2014). For instance, aberrant methylation of the MDR1 promoter is related to structural variations of chromatin and transcriptional repression (Baker and El-Osta, 2003). Similarly, long-term use of 5-Azacytidine (AZA) like DNMTi acquires resistance (Singh and Yu, 2018). However, small inhibitors targeting UHRF1, promote the sensitivity of therapeutics and elevate cancer inhibition (Abdullah et al., 2021).

Hemimethylated CpG sites are target sequences for the maintenance of DNA methylation and become completely methylated by UHRF1. Among other domains, The SET and RING-associated (SRA) domain of UHRF1 identifies the 5-methylcytosine (5 mC) in hemimethylated CpG sequences (Arita et al., 2008; Avvakumov et al., 2008; Hashimoto et al., 2008; Qian et al., 2008; Frauer et al., 2011). The SRA domain recognizes the presence of methylated cytosine and regulates the recruitment of DNMT1 (Arita et al., 2008; Hashimoto et al., 2008; Qian et al., 2008; Frauer et al., 2011; Bronner, Krifa and Mousli, 2013). Indeed, the SRA domain shows direct interaction with DNMT1 and catalyzes the methylation function (Berkyurek et al., 2014). It has been shown that the activity of DNMT1 has been accelerated by 1.9-fold due to the SRA domain and 5-fold because of UHRF1 (Bashtrykov et al., 2014). Therefore, the SRA domain has been identified as a potential target for inhibiting the aberrant global DNA methylation (Bashtrykov et al., 2014). Natural small molecules would not only a promising therapeutics against the SRA domain but also can possess the least side effects as anti-cancer drugs (Das and Singal, 2004).

Beyond the traditional drug discovery strategy, *in-silico* drug design has gained the attraction of concern due to time and cost management (Lin, Li and Lin, 2020). In contrast, natural chemical extraction and characterization for anticancer drug development are frequently time-consuming and include several inevitable barriers (Fang et al., 2018). Computer-aided drug design (CADD) solves this constraint by making it simple to screen, identify, and describe novel drug candidates within a short amount of time (Ahammad et al., 2019). CADD-mediated therapeutic development against lung and prostate cancer, for example, has been previously reported (Cui et al., 2020). Molecular docking and molecular dynamics (MD) simulation-based approaches are used in the CADD study to find viable therapies for various diseases (Lu et al., 2018; Shukla et al., 2021). Molecular docking analysis aids in the first screening of medication candidates for favorable binding capacity to drug-like ligands to the intended target (Kitchen et al., 2004). Similarly, MD simulations aid in understanding the stability of protein-ligand interactions in a synthetic environment that mimics the human body's environment (Singh and Bharadvaja, 2021). As a

result, computational drug design methodologies were used in this investigation to help screen out possible therapeutic candidates against the SRA domain of the UHRF1 protein.

Previously, chicoric acid—a phenolic compound derived from various plants (Lee and Scagel, 2013) has been reported as it may be useful in NASH and liver fibrosis treatment (Kim et al., 2017; Pan et al., 2020). Chicoric acid as a bioactive anticancer drug in colorectal cancer has been also reported (Tsai et al., 2012). However, as an epi-drug the role of chicoric acid was overlooked. Hence, the present study is aimed to investigate the role of chicoric acid in targeting UHRF1.

MATERIALS AND METHODS

Preparation of PDB Structures

The crystal structure of the SRA domain of E3 ubiquitin-protein ligase UHRF1 (c) was downloaded from the Protein Data Bank [RCSB PDB: Homepage. Available online: <https://www.rcsb.org/> (Accessed on 25 March 2022).], the protein is then prepared and optimized by using the “Protein preparation wizard” tool of Schrödinger suite (Schrödinger, L. Schrödinger Release 2021-4: Protein Preparation Wizard; Epik, Schrödinger, LLC, New York, NY, 2021). The hydrogen bonds were added, metal bonds were deleted, zero-order bonds were added between metals and nearby atoms, and correction of the formal charges to metals and neighboring atoms was done. Then add and optimize the missing side chain by running a prime job, then generate protonation and metal charge for states for the ligands, cofactors, and metals at 7.0 ± 2.0 pH. Finally, H-bonds of hydroxyl, Asn, Gln, and His are optimized at pH 7.0 using PROPKA (Olsson et al., 2011), removal of water molecules beyond 3 Å from HET groups and OPLS4 force field has been used for minimization.

Data Retrieval and Ligand Preparations

The natural organic compound library was retrieved from Selleckchem (<https://www.selleckchem.com>) as an SDF file ‘20210416-L7600-Natural-Organic-Compound-Library.sdf’ on 25 April 2021. The sdf file contained 1,126 natural organic compounds; of these, only 774 were found to have 3D structures when searched in PubChem. The 774 compounds were further filtered based on molecular weight (<500), and finally, 709 compounds were obtained and selected for virtual screening. The selected compounds were prepared using LigPrep (Schrödinger Release 2021-4: LigPrep, Schrödinger, LLC, New York, NY, 2021), 2D structures were converted to 3D, and their tautomeric forms and ionization states were generated.

Receptor Grid Generation and Docking

Glide (Schrödinger, L. Schrödinger Release 2021-4: Glide, Schrödinger, LLC, New York, NY, 2021) was utilized for both grid generation and ligands docking. The grid was generated using the PDB: 3BI7. The binding region was specified by picking the entry identified using the SiteMap program (Schrödinger Release 2021-4: SiteMap, Schrödinger, LLC, New York, NY, 2021). The partial charge cut-off and non-polar atoms (VdW

radii scaling factor) like parameters were set as 0.25 and 0.1, respectively. Molecular docking simulation has been performed by using the “ligand docking” tool in the Schrödinger suite. The selected protocol was Extra precision (XP), the ligand sampling method was flexible, and all the other settings were kept as default.

Molecular Dynamics Simulations

Molecular dynamics (MD) simulation has been performed by using Schrödinger suite (Schrödinger, L. Schrödinger Release 2021-4: Desmond Molecular Dynamics System, D. E. Shaw Research, New York, NY, 2021. Maestro-Desmond Interoperability Tools, Schrödinger, New York, NY, 2021), the systems of Chicoric acid (CID: 5281764) in complex with 3BI7 and Nystose (CID: 166775) were retrieved from the results of docking and first tuned through the “System Builder” tool. The orthorhombic-shaped box and TIP3P as the solvent model has been chosen. The neutralization of the system has been done with Na^+ ions additions. Also, the slide distances box was fixed at 10 Å. 100 ns/trajectory has been set up for the MD calculation while constantly maintaining pressure, temperature, and the number of atoms. The pressure and temperature have been set at 1.01325 bar and 300.0 K, with the OPLS4 force field.

In Silico Toxicity Analysis

To investigate the toxicity of chicoric acid through *in silico* analysis we availed the ProToxII web server (https://tox-new.charite.de/protox_II/) (65). The ProTox-II web server integrates several criteria like molecular similarity, pharmacophores, fragment propensities, and machine-learning models to predict various toxicity endpoints like-cytotoxicity, hepatotoxicity, carcinogenicity, mutagenicity, immunotoxicity, adverse outcomes pathways, etc.

Cell Culture and Dose Determination

The HCT116 cell line was collected by Dr. Imran’s Lab, Dept. of Biochemistry, KAU, Jeddah. The cell culture was performed in Dulbecco’s modified Eagle’s medium (UFS Biotech, Riyadh, KSA) supplemented with 10% FBS and 1% penicillin (Invitrogen) and incubated at 37°C. The cells were maintained up to 80–90% confluence and checked regularly to avoid any *Mycoplasma* contamination (Shait Mohammed et al., 2021). Upon confluence, cells were trypsinized and seeded in 6-well plates and incubated overnight to ensure that cells were healthy without any contamination. The next day the seeded cells were randomly treated with chicoric acid at 2.5, 5 and 7.5 μM concentrations.

Extraction of Genomic DNA

The genomic DNA was isolated from both control (untreated) and treated HCT116 cells line by utilizing DNABler kit (<https://havensci.com/>; Lot no. DE95050). 200 μL of digestion buffer was added to each sample. 20 μL of RNase A and Proteinase K were added. Afterward, the samples were vortexed and incubated in a heat block (~60°C). Then 200 μL of lysis buffer was added followed by vortexing and centrifugation. 99% ethanol was added to aliquots. Next, ethanol-lysis buffer mix samples were



collected in a spin column (nuclease-free) for further centrifugation at 10,000 g speed. After centrifugation, the samples were washed by wash buffer by following the supplied protocol of the manufacturer. 50 μ L elution buffer was added to the center of the column and incubated the column at room temperature for 2 min. Then centrifugation was done to elute the genomic DNA at a speed of 8000 g for 2 min (Khan et al., 2022).

Global Methylation (5 mC%) Level Determination

The global methylation (5 mC) level of the targeted HCT116 cell line was determined by using MethylFlash™ global DNA methylation (5-mC) ELISA Easy Kit (Catalog no. P-1030) in both treated and untreated conditions. 200 ng of DNA from each sample was collected and used for the experimental analysis. The binding solution was added to the extracted DNA samples in wells. After that, 5 mC antibody, developer solution, and stop solution were added as per manufacturer protocol. The optical density (OD) was determined at the end at 450 nm wavelength by using BioTek ELISA microplate reader (Khan et al., 2022).

RESULTS

Molecular Docking Studies

Since the crystal structure of the SRA domain of E3 ubiquitin-protein ligase UHRF1(PDB: 3BI7) doesn't contain ligands/inhibitors, and to define the Grid box, we decided to perform site mapping to identify the potential binding sites on the protein. The SiteMap program [Schrödinger Release 2021-4:

SiteMap, Schrödinger, LLC, New York, NY, 2021.] detect only one site, as shown in **Figure 1**. Then, a grid box is generated around the detected protein's binding site of the minimized protein by using a receptor-Grid-Generation tool in Maestro. The obtained Ligiprep file that contains 3D molecular structures of the selected compounds was docked into the protein binding site. **Table 1** showed the docked ligands' results that were selected due to their most negative docking scores, and these scores demonstrated the best-bonded ligand with relative binding affinities and conformations. Chicoric acid (CID: 5281764) and Nystose (CID: 166775) displayed the highest negative docking scores of -13.041 and -12.962 kcal/mol in complex with 3BI7, respectively. The molecular docking results showed that the chicoric acid bound well within the binding site (**Figures 2A,B**) with the highest negative docking scores of -13.041 and inter-acted within 3 Å with 14 residues: Ala-463, Gly-464, Gly-465, Tyr-466, Asp-469, Ser-571, Val-575, Gln-499, Gly-483, Gly-482, Ser-481, Gly-480, Thr-479, Tyr-478, (**Figures 2C,D**). Chicoric acid form charged negative interaction with Asp-469; polar interaction with Ser-571, Gln 499, Ser 481, Thr-479; hydrophobic interaction with Ala 463, Tyr-466, Val-575, Tyr-478; Also form hydrogen bond donor interaction with Gly-464 Asp-469, Gly-482, Thr-479; and hydrogen bond acceptor interaction with Tyr-466, Gln 482.

Since the molecular docking results showed that the Nystose bound well within the binding site (**Figures 3A,B**) with second-highest negative docking scores of -12.962 and interacted within 3 Å with 16 residues: Arg-433, Gly-448, Val-446, Val-461, Leu-462, Ala-463, Gly-464, Gly-465, Tyr-466, Asp-469, Tyr-478, Thr-479, Gly-480, Ser-481, Gly-482, Gln-499 (**Figures 3C,D**). Nystose form charged negative interaction with Asp-469; charged positive interaction with Arg-433; polar interaction with Gln 499, Ser 481, Thr-479; hydrophobic interaction with Ala 463, Tyr-466, Val-446, Val-461, Leu-462, Tyr-478; Also form hydrogen bond donor interaction with Val-446, Val-461, Asp-469, Thr-479, Gly-480, Gly-482; and hydrogen bond acceptor interaction with Ala-463, Tyr-466.

Molecular Dynamics Simulation

The MD simulations are performed to simulate the aqueous physiological environment to assess the changes in protein conformation and binding affinity during the simulation time, compared to the original affinity and confirmation of the crystal structure (Hollingsworth and Dror, 2018). Therefore, the MD study was performed using Desmond software [Schrödinger Release 2021-4: Desmond Molecular Dynamics System, D. E. Shaw Research, New York, NY, 2021.] to evaluate the binding affinity and stability of the protein-ligand complexes at pH 7.0 \pm 0.2 over 100 ns. Only the two top-scoring compounds in the docking study, i.e., Chicoric acid (CID: 5281764) and Nystose (CID: 166775), were analyzed by MD. The RMSD maps of the selected compounds complexed with the SRA domain of E3 ubiquitin-protein ligase UHRF1(PDB: 3BI7) measure the average change in the positions of the atoms of the protein and ligand inside. For

TABLE 1 | In silico screening/docking results of the docked ligands that were selected owing to their most negative docking scores, with SRA domain of E3 ubiquitin-protein ligase UHRF1(PDB: 3BI7).

^a Compounds CID	Docking Score	Glide g-score	Glide e-model	XP GScore
5281764 (Chicoric acid)	-13.041	-65.303	-13.041	-13.041
166775 (Nystose)	-12.962	-60.686	-12.962	-12.962
439531	-11.978	-63.731	-11.978	-11.978
10542	-10.866	-52.983	-10.866	-10.866
5280805	-9.836	-71.019	-9.836	-9.836
5281377	-9.606	-60.709	-9.606	-9.606
4789	-10.358	-67.504	-10.358	-10.358
4789	-9.628	-61.404	-9.628	-9.628
83489	-9.374	-68.28	-9.374	-9.374
439242	-9.373	-55.967	-9.373	-9.373
6134	-9.29	-49.674	-9.29	-9.29
92817	-9.245	-59.163	-9.245	-9.245
5280704	-9.112	-65.2	-9.112	-9.112
11458	-9.013	-47.5	-9.013	-9.013
65064	-9.055	-66.577	-9.055	-9.055
160469	-8.937	-47.311	-8.937	-8.937
3085296	-8.91	-53.671	-8.91	-8.91
9476	-8.895	-49.356	-8.895	-8.895
6443665	-9.093	-58.108	-9.093	-9.093
10712	-8.67	-50.74	-8.67	-8.67
73191	-8.585	-58.472	-8.585	-8.585
5281544	-8.541	-51.528	-8.541	-8.541
5481663	-8.558	-77.148	-8.558	-8.558
65064	-9.974	-66.823	-9.974	-9.974
73395	-8.468	-68.725	-8.468	-8.468
87691	-8.338	-46.766	-8.338	-8.338
73568	-10.384	-69.056	-10.384	-10.384
125153	-8.221	-84.2	-8.221	-8.221
656569	-8.212	-44.998	-8.212	-8.212
440660	-8.207	-56.717	-8.207	-8.207
5282151	-8.145	-61.64	-8.145	-8.145
73466	-8.065	-43.983	-8.065	-8.065
736	-8.038	-36.572	-8.038	-8.038
503737	-8.015	-60.238	-8.015	-8.015

^aIdentifier from PubChem database of chemical molecules and their activities in biological assays.

compound Chicoric acid, the RMSD of the protein and Chicoric acid laid over each other, indicating increased stability of the UHRF1-Chicoric acid complex (**Figure 4A**). Additionally, the fluctuation seen for both over the 100 ns was within the range. A similar RMSD pattern was observed for Nystose and UHRF1 complex, despite the sudden, non-significant fluctuation of Nystose at around 80 ns (**Figure 5A**).

The secondary structure of UHRF1(PDB: 3BI7) was also evaluated throughout the simulation while complexed with each ligand. **Figures 4B**, **Figure 5B** represented the protein evaluation while complexed with Chicoric acid and Nystose. The top plot showed the distribution of the SSE (α -helices and β -sheets) throughout the protein, represented by the residue index. The middle plot monitored the overall %SSE, while the bottom plot evaluated each SSE throughout the simulation. Both plots indicated that the overall %SSE of the protein was maintained, and each SSE was stable over the simulation.

The MD study also evaluated the binding interactions of a protein-ligand complex. For the ligand Chicoric acid, the bar graph represented what type(s) of interactions the amino acid

residues in the binding pocket made with the ligand and for how long the interaction was maintained throughout the simulation. The interactions were color-coded in the stacked bar graph, as indicated in **Figure 6A**. Asp-467 made direct H-bonding and through water bridges with Chicoric acid and had a normalized value of ~ 1.2 . The value > 1 represented the combined value of >1 type of interaction, indicating that these interactions were maintained for $\sim 120\%$ of the simulation time. The other vital interactions were Gly-464, Glu-467, Tyr-478, Thr-479, Gly-480, and Ser-571, with value of ~ 0.7 , ~ 0.76 , ~ 0.8 , ~ 0.82 , ~ 0.95 , and ~ 0.6 , respectively. **Figure 6B** showed only the interactions between Chicoric acid and the protein that occurred $\geq 30\%$ of the simulation time. **Figure 6C** displayed the specific interactions between ligand Chicoric acid and the protein (top plot). At the same time, the bottom panel demonstrated the protein residues that interacted with the ligand at each time point/trajectory. If a residue makes more than one specific interaction with the ligand, it appears as darker orange color in the plot. As mentioned earlier, Asp-469 made >1 interaction with the ligand, represented by the dark orange color in the plot throughout the trajectory.

Figure 7 shows the amino acid residues of the protein binding pocket that interacted with Nystose. Val-446, Ala-463, and Thr-479

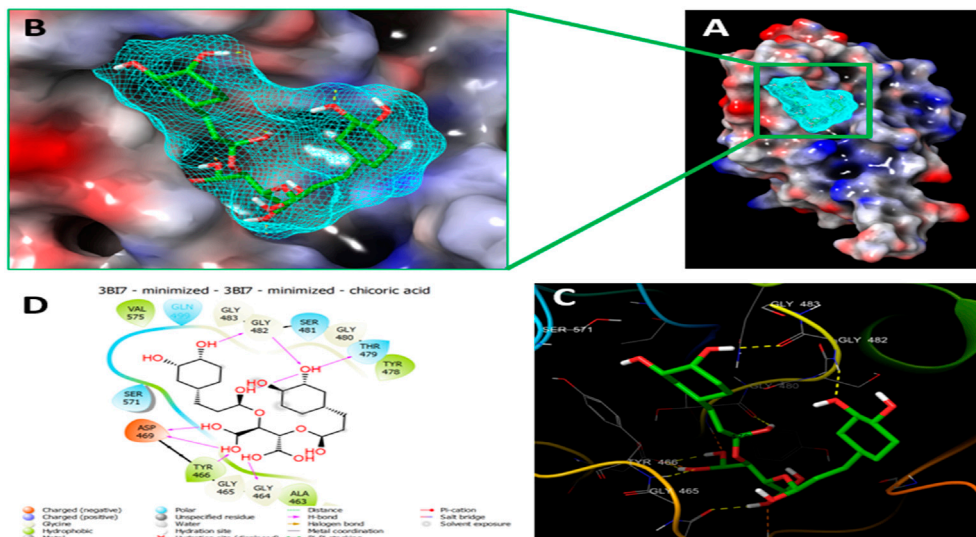


FIGURE 2 | Molecular Docking of chicoric acid with UHRF1. **(A)** Molecular surface display with an electrostatic potential color scheme for UHRF1-Chicoric acid complex and the close-up view presented. **(B)** Putative binding mode of Chicoric acid in the binding site of UHRF1 (PDB: 3BI7) **(C)** Chicoric acid was displayed as green ball-and-sticks. And the amino acid residues of the are represented as grey sticks, and H-bonds are described in yellow dotted lines. **(D)** 2D depiction of the ligand-protein interactions.

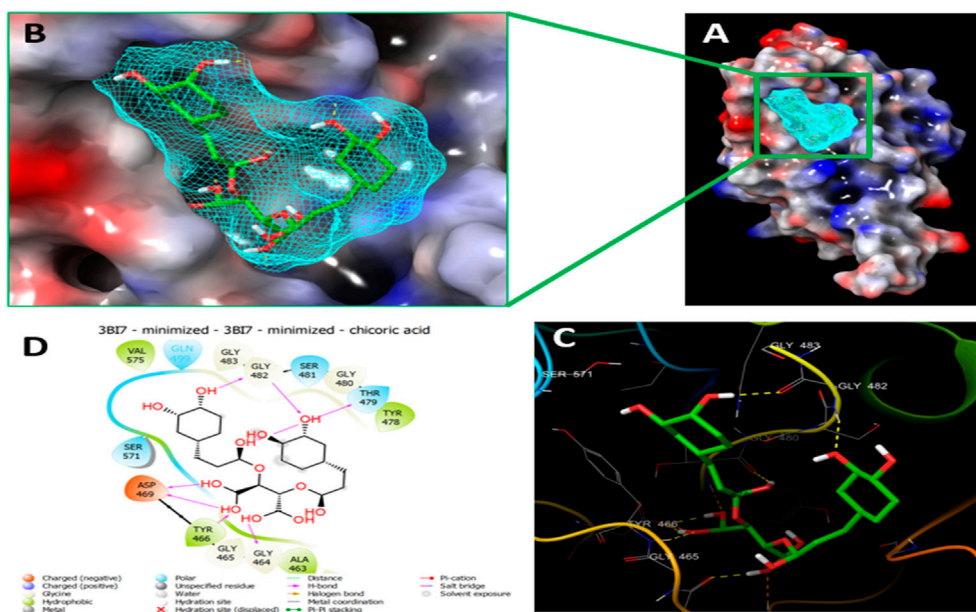
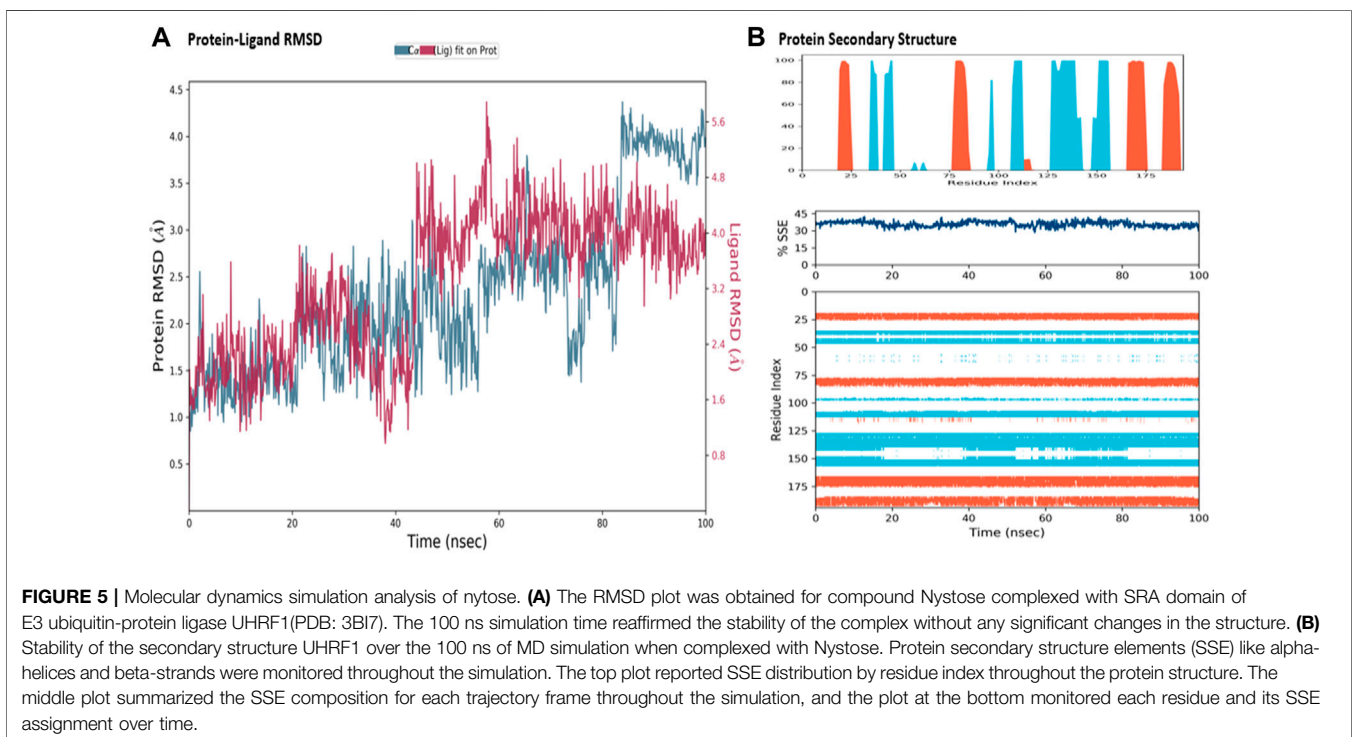
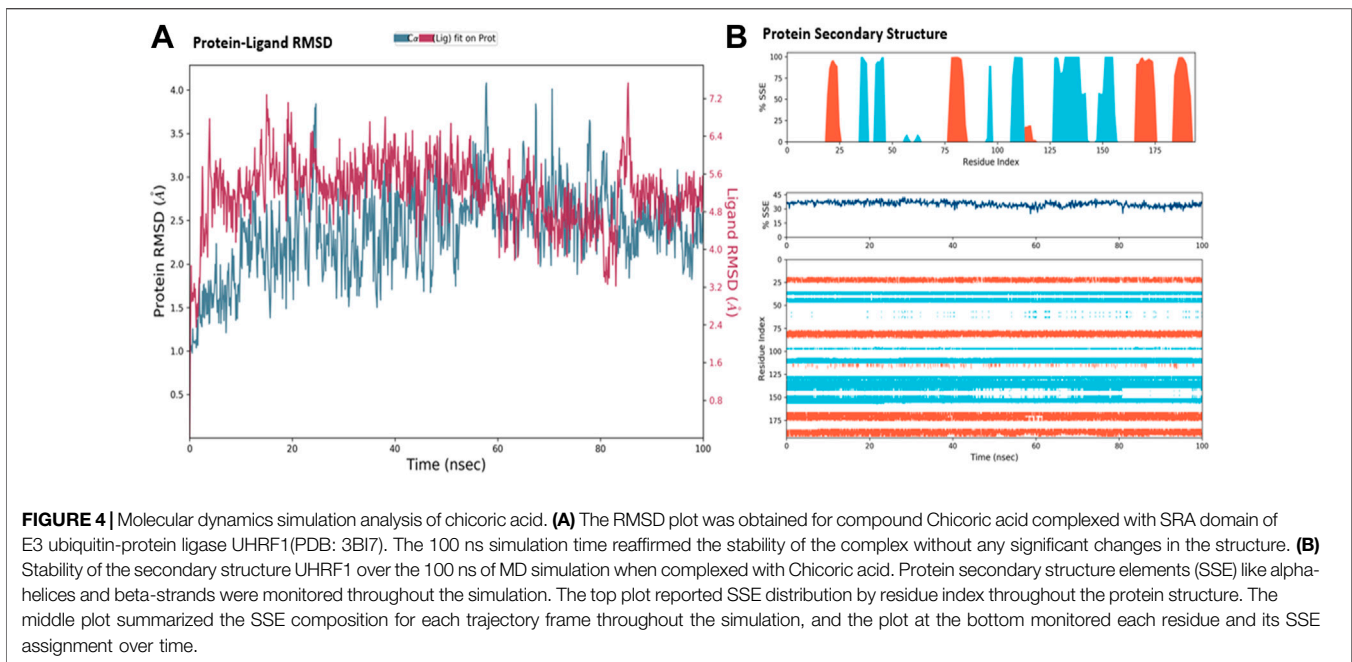


FIGURE 3 | Molecular Docking of nystose with UHRF1. **(A)** Molecular surface display with an electrostatic potential color scheme for UHRF1 - Nystose complex and the close-up view presented. **(B)** Putative binding mode of Nystose in the binding site of UHRF1 (PDB: 3BI7) **(C)** Nystose was displayed as green ball-and-sticks. And the amino acid residues of the binding site are represented as grey sticks, and H-bonds are expressed in yellow dotted lines. **(D)** 2D depiction of the lig-and-protein interactions.

made direct H-bonding, and through water, bridges with Nystose had a normalized value of ~ 0.94 , ~ 1.50 , and ~ 1.63 . The other vital interactions were with Arg-433, Gly-464, Asp-469, Gly-480, and Gly-482, with values of ~ 0.82 , ~ 0.96 , ~ 1.38 , ~ 0.77 ~ 0.82 , respectively.

Analysis of *In Silico* Toxicity

Our *in-silico* toxicity results for chicoric acid nystose showed that the compounds belong to the toxicity class 5 with LD50 of 5000 mg/kg and 3000 mg/kg respectively. The various toxicity



model reports that include hepatotoxicity, carcinogenicity, stress response pathways, etc, were depicted and represented in **Table 2**.

Global Methylation Level Reduced by Chicoric Acid

The level of global methylation (5mC) in HCT116 cell line was determined by using the computationally identified chicoric

acid. Based on a previous study (Sun et al., 2019), the methylation level was calculated at three different doses of chicoric acid, such as 2.5, 5 and 7.5 μM . Moreover, 5Azacytidine (as a positive control of DNMTi) treatment was also performed for assessing the %5 mC level (Nur et al., 2022). The data illustrated that a 2.5 μM dose had a very low effect on the 5 mC level reduction relative to the control sample. Moreover, the methylation (5mC) level was moderately

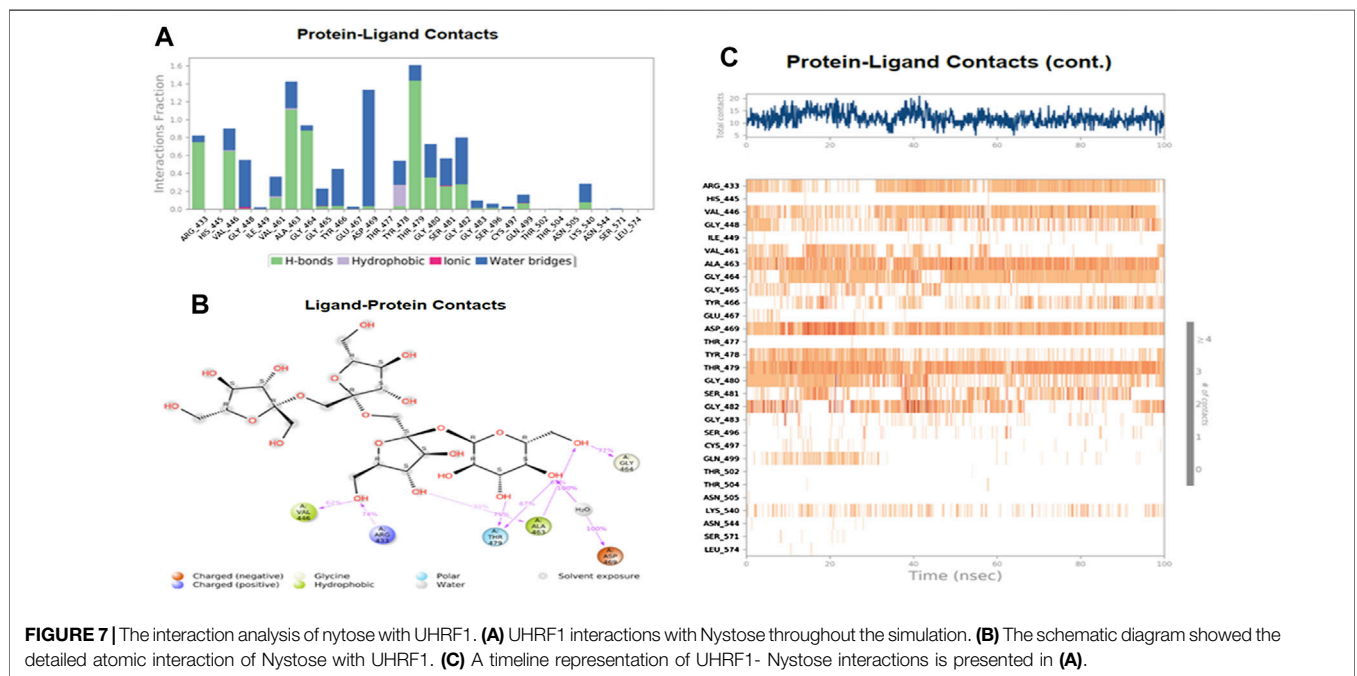
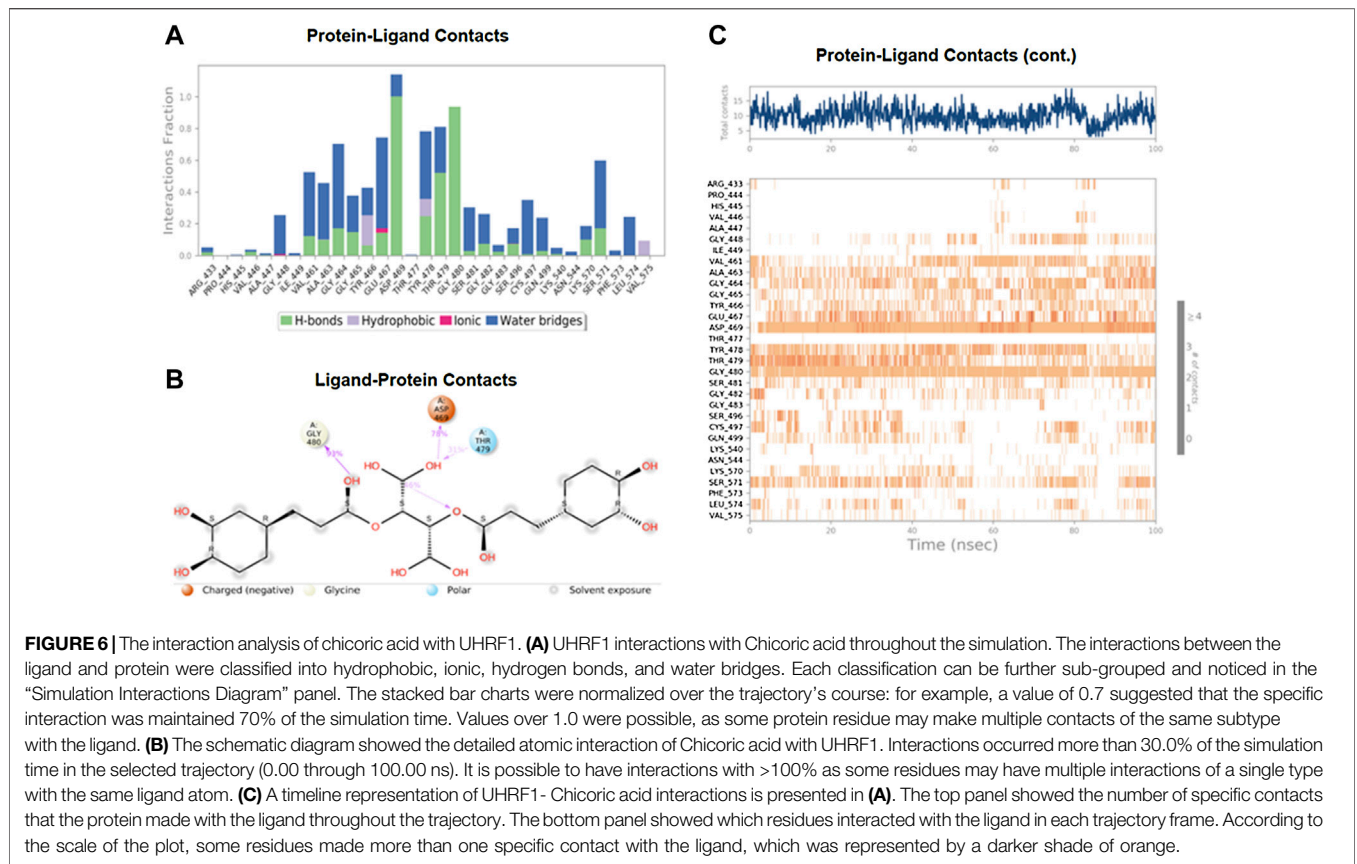
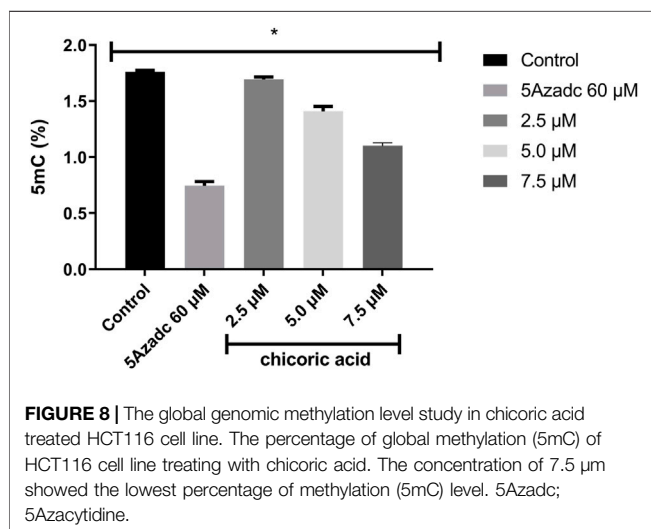


TABLE 2 | Toxicity analysis of chicoric acid with different parameters such as, organ toxicity, toxicity endpoints, and signaling and response pathways.

Classification	Target	Chicoric acid	Nystose
Oral toxicity	LD50 (mg/kg)	5000	3000
Organ toxicity	Hepatotoxicity	Inactive	Inactive
Toxicity end points	Carcinogenicity	Inactive	Inactive
	Immunotoxicity	Active	Inactive
	Mutagenicity	Inactive	Inactive
	Cytotoxicity	Inactive	Inactive
	Aryl hydrocarbon Receptor (AhR)	Inactive	Inactive
Tox21-Nuclear receptor signalling pathways	Androgen Receptor (AR)	Inactive	Inactive
Tox21-Nuclear receptor signalling pathways	Androgen Receptor Ligand Binding Domain (AR-LBD)	Inactive	Inactive
Tox21-Nuclear receptor signalling pathways	Aromatase	Inactive	Inactive
Tox21-Nuclear receptor signalling pathways	Estrogen Receptor Alpha (ER)	Inactive	Inactive
Tox21-Nuclear receptor signalling pathways	Estrogen Receptor Ligand Binding Domain (ER-LBD)	Inactive	Inactive
Tox21-Nuclear receptor signalling pathways	Peroxisome Proliferator Activated Receptor Gamma (PPAR-Gamma)	Inactive	Inactive
Tox21-Stress response pathways	Nuclear factor (erythroid-derived 2)-like 2/antioxidant responsive element (nrf2/ARE)	Inactive	Inactive
Tox21-Stress response pathways	Heat shock factor response element (HSE)	Inactive	Inactive
Tox21-Stress response pathways	Mitochondrial Membrane Potential (MMP)	Inactive	Inactive
Tox21-Stress response pathways	Phosphoprotein (Tumor Suppressor) p53	Inactive	Inactive
Tox21-Stress response pathways	ATPase family AAA domain-containing protein 5 (ATAD5)	Inactive	Inactive



decreased by 5 μM chicoric acid treatment. However, 7.5 μM chicoric acid treatment significantly reduced the 5 mC level by around 0.6% compared to the control (Figure 8).

DISCUSSION

DNMTs have profound epigenetic effects on various tumorigenic and non-tumorigenic cells (Robertson, 2001). Besides a coordinating protein like UHRF1 interact with DNMTs through SAR domain. Previously, it has been shown that targeting the SRA domain of UHRF1 with various natural compounds provide a promising strategy for chemotherapeutic purpose in cancer cell lines (Patnaik et al., 2018). However, the study of targeting the SRA domain of UHRF1 by chicoric acid has been overlooked previously. Hence, in our present study, we aimed to investigate this gap. First, we retrieved the natural compounds library followed by virtual

screening through molecular docking simulation. In molecular docking simulation, we virtually screened 709 natural organic compounds against the SRA domain of UHRF1. After molecular docking simulations, we selected the top two compounds based on the docking score which include chicoric acid and nystose. The molecular docking simulation result of chicoric acid showed that the chicoric acid interacted with 14 amino acids of SRA domain UHRF1 whereas nystose interacted with 16 residues including Asp469 residue. Asp469 of SRA domain is studied as an active residue that recognizes methylcytosine (Patnaik, 2020). The study showed that chicoric acid formed significant interactions with Asp469 while the interaction with nystose is very low. Furthermore, the study utilized molecular dynamics simulation to analyze the protein-ligand complex stability (Islam et al., 2022). Also, MD simulation calculates the RMSD values to confirm the interaction stability and rigidity of the compounds with the target protein (Liu et al., 2017). The RMSD value of the SRA domain-chicoric acid complex showed more stable considerably. Besides the interaction mapping also chicoric acid confirmed more stable and durable H-bonding with Asp469 residue throughout 100ns simulation. Moreover, we also investigated the *in-silico* toxicity test that showed both chicoric acid and nystose meet all the safety parameters and belong to toxicity class 5. However, chicoric acid has been characterized as a more selective candidate with a higher LD50 value of 5000 mg/kg. Previously, chemoinformatics study of chicoric acid has been studied targeting various proteins (Healy et al., 2009; Baskaran et al., 2012; Li et al., 2021). Till now no chemoinformatics study of chicoric acid-targeting SRA domain of UHRF1 has been elucidated.

Additionally, the global methylation level (5mC%) was measured to validate our *in-silico* results (De Oliveira et al., 2020). We tested the chicoric acid on the HCT116 cell line at 2.5, 5 and 7.5 μM doses. From the treated sample we have extracted the genomic DNA to measure the global methylation level of the genome (5mC%). Our results showed that at 7.5 μM treatment chicoric acid reduced the highest level of 5mC. No previous study showed the effect of chicoric acid on global methylation levels.

CONCLUSION

DNA methylation is necessary to control the mammalian genome expression and stability. However, aberrant DNA methylation leads to carcinogenesis. UHRF1 is found as a crucial target for facilitating uncontrolled methylation. Particularly, SRA domain of UHRF1 is highly responsive to incorporating other epigenetic writers including DNMT1. Therefore, our study utilized diverse *in-silico* approaches and virtually screened 709 natural compounds that showed chicoric acid and ntyose as prominent interactors with or without the SRA domain of UHRF1 protein and finally identified chicoric acid as a promising drug candidate against the SRA domain. Finally, chicoric acid justified the epi-drug-like effect of chicoric acid on HCT116 cancer cell line by measuring the global methylation level (5mC%). Chicoric acid was substantially effective in reducing DNA methylation levels suggesting that chicoric acid may become a new epigenetic inhibitory drug for chemotherapeutic purposes in cancer treatment.

DATA AVAILABILITY STATEMENT

The raw data supporting the conclusion of this article will be made available by the authors, without undue reservation.

REFERENCES

- Abdullah, O., Omran, Z., Hosawi, S., Hamiche, A., Bronner, C., and Alhosin, M. (2021). Thymoquinone Is a Multitarget Single Epidrug that Inhibits the UHRF1 Protein Complex. *Genes* 12 (5), 622. doi:10.3390/GENES12050622
- Ahamed, M., Akhtar, M. J., Khan, M. A. M., and Alhadlaq, H. A. (2022). Enhanced Anticancer Performance of Eco-Friendly-Prepared Mo-ZnO/RGO Nanocomposites: Role of Oxidative Stress and Apoptosis. *ACS Omega* 7 (8), 7103–7115. doi:10.1021/ACSOMEGA.1C06789/ASSET/IMAGES/LARGE/AO1C06789_0014.JPG
- Ahamed, M., Akhtar, M. J., Khan, M. M., and Alhadlaq, H. A. (2021). SnO₂-Doped ZnO/Reduced Graphene Oxide Nanocomposites: Synthesis, Characterization, and Improved Anticancer Activity via Oxidative Stress Pathway. *Int. J. Nanomedicine* 16, 89–104. doi:10.2147/IJN.S285392
- Ahmad, F., Tengku Abd Rashid, T. R., Mohamed, M., Tanbin, S., and Ahmad Fuad, F. A. (2019). Contemporary Strategies and Current Trends in Designing Antiviral Drugs against Dengue Fever via Targeting Host-Based Approaches. *Microorganisms* 7 (9), 296. doi:10.3390/MICROORGANISMS7090296
- Alhosin, M., Omran, Z., Zamzami, M. A., Al-Malki, A. L., Choudhry, H., Mousli, M., et al. (2016). Signalling Pathways in UHRF1-dependent Regulation of Tumor Suppressor Genes in Cancer. *J. Exp. Clin. Cancer Res.* 35 (1), 1–11. doi:10.1186/S13046-016-0453-5
- Arita, K., Ariyoshi, M., Tochio, H., Nakamura, Y., and Shirakawa, M. (2008). Recognition of Hemi-Methylated DNA by the SRA Protein UHRF1 by a Base-Flipping Mechanism. *Nature* 455 (7214), 7214455818–7214455821. doi:10.1038/nature07249
- Avvakumov, G. V., Walker, J. R., Xue, S., Li, Y., Duan, S., Bronner, C., et al. (2008). Structural Basis for Recognition of Hemi-Methylated DNA by the SRA Domain of Human UHRF1. *Nature* 455 (7214), 822–825. doi:10.1038/NATURE07273
- Baker, E. K., and El-Osta, A. (2003). The Rise of DNA Methylation and the Importance of Chromatin on Multidrug Resistance in Cancer. *Exp. Cell Res.* 290 (2), 177–194. doi:10.1016/S0014-4827(03)00342-2
- Bashtrykov, P., Jankevicius, G., Jurkowska, R. Z., Ragozin, S., and Jeltsch, A. (2014). The UHRF1 Protein Stimulates the Activity and Specificity of the Maintenance DNA Methyltransferase DNMT1 by an Allosteric Mechanism. *J. Biol. Chem.* 289 (7), 4106–4115. doi:10.1074/JBC.M113.528893

AUTHOR CONTRIBUTIONS

MIK and MR conceptualized, MAA, SMN, AKAK and MR performed methodology and software, SBIH and HC performed validation, AA and MIK performed formal analysis, HC and SBIH managed the resources and funding acquisitions, MR performed data curation, MAA and SMN prepared manuscript writing, MIK reviewed and edited manuscript writing.

FUNDING

The authors extend their appreciation to the Deputyship for Research and Innovation, Ministry of Education in Saudi Arabia, for funding this research work through the project number IFPRC-193-130 2020, and King Abdulaziz University DSR, Jeddah, Saudi Arabia.

ACKNOWLEDGMENTS

The authors would like to thank the Department of Biochemistry, King Abdulaziz University.

- Baskaran, S. K., Goswami, N., Selvaraj, S., Muthusamy, V. S., and Lakshmi, B. S. (2012). Molecular Dynamics Approach to Probe the Allosteric Inhibition of PTP1B by Chlorogenic and Cichoric Acid. *J. Chem. Inf. Model.* 52 (8), 2004–2012. doi:10.1021/CI200581G
- Baylin, S. B., Esteller, M., Rountree, M. R., Bachman, K. E., Schuebel, K., and Herman, J. G. (2001). Aberrant Patterns of DNA Methylation, Chromatin Formation and Gene Expression in Cancer. *Hum. Mol. Genet.* 10 (7), 687–692. doi:10.1093/HMG/10.7.687
- Baylin, S. B., and Jones, P. A. (2016). Epigenetic Determinants of Cancer. *Cold Spring Harb. Perspect. Biol.* 8 (9), a019505. doi:10.1101/CSHPERSPECT.A019505
- Beck, A., Trippel, F., Wagner, A., Joppien, S., Felle, M., Vokuhl, C., et al. (2018). Overexpression of UHRF1 Promotes Silencing of Tumor Suppressor Genes and Predicts Outcome in Hepatoblastoma. *Clin. Epigenet.* 10 (1), 27. doi:10.1186/S13148-018-0462-7
- Berkyurek, A. C., Suetake, I., Arita, K., Takeshita, K., Nakagawa, A., Shirakawa, M., et al. (2014). The DNA Methyltransferase Dnmt1 Directly Interacts with the SET and RING Finger-Associated (SRA) Domain of the Multifunctional Protein Uhrf1 to Facilitate Accession of the Catalytic Center to Hemi-Methylated DNA. *J. Biol. Chem.* 289 (1), 379–386. doi:10.1074/JBC.M113.523209
- Bird, A. P., and Wolffe, A. P. (1999). Methylation-Induced Repression- Belts, Braces, and Chromatin. *Cell* 99 (5), 451–454. doi:10.1016/S0092-8674(00)81532-9
- Bonapace, I. M., Latella, L., Papait, R., Nicassio, F., Sacco, A., Muto, M., et al. (2002). Np95 Is Regulated by E1A during Mitotic Reactivation of Terminally Differentiated Cells and Is Essential for S Phase Entry. *J. Cell Biol.* 157 (6), 909–914. doi:10.1083/JCB.200201025
- Bostick, M., Kim, J. K., Estève, P.-O., Clark, A., Pradhan, S., and Jacobsen, S. E. (2007). UHRF1 Plays a Role in Maintaining DNA Methylation in Mammalian Cells. *Science* 317 (5845), 1760–1764. doi:10.1126/SCIENCE.1147939
- Bronner, C., Achour, M., Arima, Y., Chataigneau, T., Saya, H., and Schini-Kerth, V. B. (2007). The UHRF Family: Oncogenes that Are Drugable Targets for Cancer Therapy in the Near Future? *Pharmacol. Ther.* 115 (3), 419–434. doi:10.1016/J.PHARMTHERA.2007.06.003
- Bronner, C., Krifa, M., and Mousli, M. (2013). Increasing Role of UHRF1 in the Reading and Inheritance of the Epigenetic Code as Well as in Tumorigenesis. *Biochem. Pharmacol.* 86 (12), 1643–1649. doi:10.1016/J.BCP.2013.10.002

- Cai, Y., Tsai, H.-C., Yen, R.-W. C., Zhang, Y. W., Kong, X., Wang, W., et al. (2017). Critical Threshold Levels of DNA Methyltransferase 1 Are Required to Maintain DNA Methylation across the Genome in Human Cancer Cells. *Genome Res.* 27 (4), 533–544. doi:10.1101/GR.208108.116
- Chen, R. Z., Pettersson, U., Beard, C., Jackson-Grusby, L., and Jaenisch, R. (1998). DNA Hypomethylation Leads to Elevated Mutation Rates. *Nature* 395 (6697), 669739589–669739593. doi:10.1038/25779
- Cheng, J., Yang, Y., Fang, J., Xiao, J., Zhu, T., Chen, F., et al. (2013). Structural Insight into Coordinated Recognition of Trimethylated Histone H3 Lysine 9 (H3K9me3) by the Plant Homeodomain (PHD) and Tandem Tudor Domain (TTD) of UHRF1 (Ubiquitin-like, Containing PHD and RING Finger Domains, 1) Protein. *J. Biol. Chem.* 288 (2), 1329–1339. doi:10.1074/JBC.M112.415398
- Crnogorac-Jurcevic, T., Gangeswaran, R., Bhakta, V., Capurso, G., Lattimore, S., Akada, M., et al. (2005). Proteomic Analysis of Chronic Pancreatitis and Pancreatic Adenocarcinoma. *Gastroenterology* 129 (5), 1454–1463. doi:10.1053/J.GASTRO.2005.08.012
- Cui, W., Aouidate, A., Wang, S., Yu, Q., Li, Y., and Yuan, S. (2020). Discovering Anti-cancer Drugs via Computational Methods. *Front. Pharmacol.* 11, 733. doi:10.3389/FPHAR.2020.00733
- Das, P. M., and Singal, R. (2004). DNA Methylation and Cancer. *J. Clin. Oncol.* 22 (22), 4632–4642. doi:10.1200/JCO.2004.07.151
- De Oliveira, N. F. P., Coêlho, M. d. C., and Viana Filho, J. M. C. (2020). ELISA Analysis of Global Methylation Levels. *Epigenetics Methods* 18, 83–92. doi:10.1016/B978-0-12-819414-0.00005-7
- Fang, J., Liu, C., Wang, Q., Lin, P., and Cheng, F. (2018). In Silico polypharmacology of Natural Products. *Briefings Bioinforma.* 19 (6), 1153–1171. doi:10.1093/BIB/BBX045
- Frauer, C., Hoffmann, T., Bultmann, S., Casa, V., Cardoso, M. C., Antes, I., et al. (2011). Recognition of 5-Hydroxymethylcytosine by the Uhrf1 SRA Domain. *PLOS ONE* 6 (6), e21306. doi:10.1371/JOURNAL.PONE.0021306
- Hashimoto, H., Horton, J. R., Zhang, X., Bostick, M., Jacobsen, S. E., and Cheng, X. (2008). The SRA Domain of UHRF1 Flips 5-methylcytosine Out of the DNA Helix. *Nature* 455 (7214), 7214455826–7214455829. doi:10.1038/nature07280
- Healy, E. F., Sanders, J., King, P. J., and Robinson, W. E. (2009). A Docking Study of L-Chicoric Acid with HIV-1 Integrase. *J. Mol. Graph. Model.* 27 (5), 584–589. doi:10.1016/J.JMGM.2008.09.011
- Hollingsworth, S. A., and Dror, R. O. (2018). Molecular Dynamics Simulation for All. *Neuron* 99 (6), 1129–1143. doi:10.1016/J.NEURON.2018.08.011
- Holohan, C., Van Schaeybroeck, S., Longley, D. B., and Johnston, P. G. (2013). Cancer Drug Resistance: an Evolving Paradigm. *Nat. Rev. Cancer* 1013 (10), 714–726. doi:10.1038/nrc3599
- Housman, G., Byler, S., Heerboth, S., Lapinska, K., Longacre, M., Snyder, N., et al. (2014). Drug Resistance in Cancer: An Overview. *Cancers* 66 (3), 17691769–17921792. doi:10.3390/CANCERS6031769
- Islam, M. R., Awal, M. A., Khames, A., Abourehab, M. A. S., Samad, A., Hassan, W. M. I., et al. (2022). Computational Identification of Druggable Bioactive Compounds from *Catharanthus roseus* and *Avicennia marina* against Colorectal Cancer by Targeting Thymidylate Synthase. *Molecules* 27 (7), 2089. doi:10.3390/MOLECULES27072089
- Jazirehi, A. R., Arle, D., and Wenn, P. B. (2012). UHRF1: a Master Regulator in Prostate Cancer. *Epigenomics* 4 (3), 251–254. doi:10.2217/EPI.12.27
- Khan, M. I., Nur, S. M., and Abdulaal, W. H. (2022). A Study on DNA Methylation Modifying Natural Compounds Identified EGCG for Induction of IFI16 Gene Expression Related to the Innate Immune Response in Cancer Cells. *Oncol. Lett.* 24 (1), 218. doi:10.3892/ol.2022.13339
- Kim, M., Yoo, G., Randy, A., Kim, H. S., and Nho, C. W. (2017). Chicoric Acid Attenuate a Nonalcoholic Steatohepatitis by Inhibiting Key Regulators of Lipid Metabolism, Fibrosis, Oxidation, and Inflammation in Mice with Methionine and Choline Deficiency. *Mol. Nutr. Food Res.* 61 (5), 1600632. doi:10.1002/MNFR.201600632
- Kitchen, D. B., Decornez, H., Furr, J. R., and Bajorath, J. (2004). Docking and Scoring in Virtual Screening for Drug Discovery: Methods and Applications. *Nat. Rev. Drug Discov.* 113 (11), 935–949. doi:10.1038/nrd1549
- Kofunato, Y., Kumamoto, K., Saitou, K., Hayase, S., Okayama, H., Miyamoto, K., et al. (2012). UHRF1 Expression Is Upregulated and Associated with Cellular Proliferation in Colorectal Cancer. *Oncol. Rep.* 28 (6), 1997–2002. doi:10.3892/OR.2012.2064
- Kong, X., Chen, J., Xie, W., Brown, S. M., Cai, Y., Wu, K., et al. (2019). Defining UHRF1 Domains that Support Maintenance of Human Colon Cancer DNA Methylation and Oncogenic Properties. *Cancer Cell* 35 (4), 633–648. doi:10.1016/J.CCELL.2019.03.003
- Lee, J., and Scagel, C. F. (2013). Chicoric Acid: Chemistry, Distribution, and Production. *Front. Chem.* 1, 40. doi:10.3389/FCHEM.2013.00040
- Li, W., Song, Y., Sun, W., Yang, X., Liu, X., and Sun, L. (2021). Both Acidic pH Value and Binding Interactions of Tartaric Acid with α -Glucosidase Cause the Enzyme Inhibition: The Mechanism in α -Glucosidase Inhibition of Four Caffeic and Tartaric Acid Derivates. *Front. Nutr.* 8, 741. doi:10.3389/FNUT.2021.766756/BIBTEX
- Li, X.-L., Xu, J. H., Nie, J. H., and Fan, S. J. (2012). Exogenous Expression of UHRF1 Promotes Proliferation and Metastasis of Breast Cancer Cells. *Oncol. Rep.* 28 (1), 375–383. doi:10.3892/OR.2012.1792
- Liao, J., Karnik, R., Gu, H., Ziller, M. J., Clement, K., Tsankov, A. M., et al. (2015). Targeted Disruption of DNMT1, DNMT3A and DNMT3B in Human Embryonic Stem Cells. *Nat. Genet.* 4747 (55), 469–478. doi:10.1038/ng.3258
- Lin, X., Li, X., and Lin, X. (2020). A Review on Applications of Computational Methods in Drug Screening and Design. *Molecules* 25 (6), 1375. doi:10.3390/MOLECULES25061375
- Liu, K., Watanabe, E., and Kokubo, H. (2017). Exploring the Stability of Ligand Binding Modes to Proteins by Molecular Dynamics Simulations. *J. Comput. Aided Mol. Des.* 31 (2), 201–211. doi:10.1007/S10822-016-0005-2/FIGURES/6
- Longley, D., and Johnston, P. (2005). Molecular Mechanisms of Drug Resistance. *J. Pathol.* 205 (2), 275–292. doi:10.1002/PATH.1706
- Lu, S., Ji, M., Ni, D., and Zhang, J. (2018). Discovery of Hidden Allosteric Sites as Novel Targets for Allosteric Drug Design. *Drug Discov. Today* 23 (2), 359–365. doi:10.1016/J.DRUDIS.2017.10.001
- Miura, M., Watanabe, H., Sasaki, T., Tatsumi, K., and Muto, M. (2001). Dynamic Changes in Subnuclear NP95 Location during the Cell Cycle and its Spatial Relationship with DNA Replication Foci. *Exp. Cell Res.* 263 (2), 202–208. doi:10.1006/EXCR.2000.5115
- Moore, L. D., Le, T., and Fan, G. (2012). DNA Methylation and its Basic Function. *Neuropsychopharmacol* 3838 (11), 23–38. doi:10.1038/npp.2012.112
- Nur, S. M., Shait Mohammed, M. R., Zamzami, M. A., Choudhry, H., Ahmad, A., Ateeq, B., et al. (2022). Untargeted Metabolomics Showed Accumulation of One-Carbon Metabolites to Facilitate DNA Methylation during Extracellular Matrix Detachment of Cancer Cells. *Metabolites* 12 (3), 267. doi:10.3390/METABO12030267
- Olsson, M. H. M., Sondergaard, C. R., Rostkowski, M., and Jensen, J. H. (2011). PROPKA3: Consistent Treatment of Internal and Surface Residues in Empirical pKa Predictions. *J. Chem. Theory Comput.* 7 (2), 525–537. doi:10.1021/CT100578Z/SUPPL_FILE/CT100578Z_SI_001.PDF
- Pan, X., Ma, X., Jiang, Y., Wen, J., Yang, L., Chen, D., et al. (2020). A Comprehensive Review of Natural Products against Liver Fibrosis: Flavonoids, Quinones, Lignans, Phenols, and Acids. *Evidence-Based Complementary Altern. Med.* 2020, 1–19. doi:10.1155/2020/7171498
- Patnaik, D., Estève, P.-O., and Pradhan, S. (2018). Targeting the SET and RING-Associated (SRA) Domain of Ubiquitin-like, PHD and Ring Finger-Containing 1 (UHRF1) for Anti-cancer Drug Development. *Oncotarget* 9 (40), 26243–26258. doi:10.18632/ONCOTARGET.25425
- Patnaik, D. (2020). Structure-based Screening of Chemical Libraries to Identify Small Molecules that Are Likely to Bind with the SET and RING-Associated (SRA) Domain of Ubiquitin-like, PHD and Ring Finger-containing 1 (UHRF1). *BMC Res. Notes* 13 (1). doi:10.1186/S13104-020-05103-4
- Pradhan, S., and Esteve, P.-O. (2003). Mammalian DNA (Cytosine-5) Methyltransferases and Their Expression. *Clin. Immunol.* 109 (1), 6–16. doi:10.1016/S1521-6616(03)00204-3
- Qian, C., Li, S., Jakoncic, J., Zeng, L., Walsh, M. J., and Zhou, M.-M. (2008). Structure and Hemimethylated CpG Binding of the SRA Domain from Human UHRF1. *J. Biol. Chem.* 283 (50), 34490–34494. doi:10.1074/JBC.C800169200
- Robertson, K. D. (2001). DNA Methylation, Methyltransferases, and Cancer. *Oncogene* 20 (24), 243139–243155. doi:10.1038/sj.onc.1204341
- Shait Mohammed, M. R., Alghamdi, R. A., Alzahrani, A. M., Zamzami, M. A., Choudhry, H., and Khan, M. I. (2021). Compound C, a Broad Kinase Inhibitor Alters Metabolic Fingerprinting of Extra Cellular Matrix Detached Cancer Cells. *Front. Oncol.* 11, 612778. doi:10.3389/FONC.2021.612778/FULL

- Sharif, J., Muto, M., Takebayashi, S.-i., Suetake, I., Iwamatsu, A., Endo, T. A., et al. (2007). The SRA Protein Np95 Mediates Epigenetic Inheritance by Recruiting Dnmt1 to Methylated DNA. *Nature* 450 (7171), 7171450908–7171450912. doi:10.1038/nature06397
- Shen, H., and Laird, P. W. (2013). Interplay between the Cancer Genome and Epigenome. *Cell* 153 (1), 38–55. doi:10.1016/J.CELL.2013.03.008
- Shukla, R., and Tripathi, T. (2021). “Molecular Dynamics Simulation in Drug Discovery: Opportunities and Challenges,” in *Innovations and Implementations of Computer Aided Drug Discovery Strategies in Rational Drug Design* (India: Springer), 295–316. doi:10.1007/978-981-15-8936-2_12
- Singh, A. K., and Yu, X. (2018). Novel Therapeutic Targeting of UHRF1 Restores 5'-Azacytidine Response in Resistant Acute Myeloid Leukemia. *Blood* 132 (Suppl. 1), 1356. doi:10.1182/BLOOD-2018-99-115735
- Singh, H., and Bharadvaja, N. (2021). Treasuring the Computational Approach in Medicinal Plant Research. *Prog. Biophysics Mol. Biol.* 164, 19–32. doi:10.1016/J.PBIOMOLBIO.2021.05.004
- Sun, X., Zhang, X., Zhai, H., Zhang, D., and Ma, S. (2019). Chicoric Acid (CA) Induces Autophagy in Gastric Cancer through Promoting Endoplasmic Reticulum (ER) Stress Regulated by AMPK. *Biomed. Pharmacother.* 118, 109144. doi:10.1016/J.BIOPHA.2019.109144
- Tsai, Y.-L., Chiu, C.-C., Yi-Fu Chen, J., Chan, K.-C., and Lin, S.-D. (2012). Cytotoxic Effects of Echinacea Purpurea Flower Extracts and Cichoric Acid on Human Colon Cancer Cells through Induction of Apoptosis. *J. Ethnopharmacol.* 143 (3), 914–919. doi:10.1016/J.JEP.2012.08.032
- Uemura, T., Kubo, E., Kanari, Y., Ikemura, T., Tatsumi, K., and Muto, M. (2000). Temporal and Spatial Localization of Novel Nuclear Protein NP95 in Mitotic and Meiotic Cells. *Cell Struct. Funct.* 25 (3), 149–159. doi:10.1247/CSF.25.149
- Unoki, M. (2011). Current and Potential Anticancer Drugs Targeting Members of the UHRF1 Complex Including Epigenetic Modifiers. *Recent Pat. anti-cancer drug Discov.* 6 (1), 116–130. doi:10.2174/157489211793980024
- Unoki, M., Daigo, Y., Koinuma, J., Tsuchiya, E., Hamamoto, R., and Nakamura, Y. (2010). UHRF1 Is a Novel Diagnostic Marker of Lung Cancer. *Br. J. Cancer* 103 (2), 217–222. doi:10.1038/SJ.BJC.6605717
- Veland, N., and Chen, T. (2017). “Mechanisms of DNA Methylation and Demethylation during Mammalian Development,” in *Handbook of Epigenetics: The New Molecular and Medical Genetics* (Texas, United States: Academic Press), 11–24. doi:10.1016/B978-0-12-805388-1.00002-X
- Yang, G.-L., Zhang, L.-H., Bo, J.-J., Chen, H.-G., Cao, M., Liu, D.-M., et al. (2012). UHRF1 Is Associated with Tumor Recurrence in Non-muscle-invasive Bladder Cancer. *Med. Oncol.* 29 (2), 842–847. doi:10.1007/S12032-011-9983-Z
- Zhang, J., Gao, Q., Li, P., Liu, X., Jia, Y., Wu, W., et al. (2011). S Phase-dependent Interaction with DNMT1 Dictates the Role of UHRF1 but Not UHRF2 in DNA Methylation Maintenance. *Cell Res.* 21 (12), 1723–1739. doi:10.1038/CR.2011.176
- Zhou, L., Zhao, X., Han, Y., Lu, Y., Shang, Y., Liu, C., et al. (2013). Regulation of UHRF1 by miR-146a/b Modulates Gastric Cancer Invasion and Metastasis. *FASEB J.* 27 (12), 4929–4939. doi:10.1096/FJ.13-233387

Conflict of Interest: AA is employed by the Translational Research Institute, Hamad Medical Corporation, Qatar.

The remaining authors declare that the research was conducted in the absence of any commercial or financial relationships that could be construed as a potential conflict of interest.

Publisher's Note: All claims expressed in this article are solely those of the authors and do not necessarily represent those of their affiliated organizations, or those of the publisher, the editors, and the reviewers. Any product that may be evaluated in this article, or claim that may be made by its manufacturer, is not guaranteed or endorsed by the publisher.

Copyright © 2022 Awal, Nur, Al Khalaf, Rehan, Ahmad, Hosawi, Choudhry and Khan. This is an open-access article distributed under the terms of the Creative Commons Attribution License (CC BY). The use, distribution or reproduction in other forums is permitted, provided the original author(s) and the copyright owner(s) are credited and that the original publication in this journal is cited, in accordance with accepted academic practice. No use, distribution or reproduction is permitted which does not comply with these terms.